J. Am. Soc. Mass Spectrom. (2016) 27:1176–1185
DOI: 10.1007/s13361-016-1390-4

RESEARCH ARTICLE

Photoleucine Survives Backbone Cleavage by Electron Transfer Dissociation. A Near-UV Photodissociation and Infrared Multiphoton Dissociation Action Spectroscopy Study

Christopher J. Shaffer,[1] Jonathan Martens,[2] Aleš Marek,[1,3] Jos Oomens,[2,4] František Tureček[1]

[1]Department of Chemistry, University of Washington, Seattle, WA 98195-1700, USA
[2]FELIX Laboratory, Radboud University Nijmegen, Institute for Molecules and Materials, Toernooiveld 7c, 6525ED, Nijmegen, The Netherlands
[3]Institute of Organic Chemistry and Biochemistry, Academy of Sciences of the Czech Republic, Prague, Czech Republic
[4]van't Hoff Institute for Molecular Sciences, University of Amsterdam, 1098XH, AmsterdamScience Park 908 The Netherlands

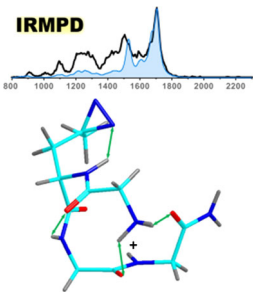

Abstract. We report a combined experimental and computational study aimed at elucidating the structure of *N*-terminal fragment ions of the ***c*** type produced by electron transfer dissociation of photo-leucine (L*) peptide ions GL*GGKX. The c_4 ion from GL*GGK is found to retain an intact diazirine ring that undergoes selective photodissociation at 355 nm, followed by backbone cleavage. Infrared multiphoton dissociation action spectra point to the absence in the c_4 ion of a diazoalkane group that could be produced by thermal isomerization of vibrationally hot ions. The c_4 ion from ETD of GL*GGK is assigned an amide structure by a close match of the IRMPD action spectrum and calculated IR absorption. The energetics and kinetics of c_4 ion dissociations are discussed.

Keywords: Peptide ions, Electron transfer dissociation, Photoleucine label, Near-UV photodissociation, Infrared multiphoton dissociation action spectroscopy

Received: 15 February 2016/Revised: 15 March 2016/Accepted: 16 March 2016/Published Online: 8 April 2016

Introduction

Photochemical labels containing the diazirine ring are useful reagents for protein footprinting [1]. Diazirine is a weak chromophore which, when photolyzed at 350–370 nm, expels a molecule of dinitrogen, creating a highly reactive carbene intermediate. The carbene can insert in a proximate X–H bond (X = C, N, O), creating a new covalent X–C bond that tags the area of contact with the diazirine ring. Photochemical diazirine-carbene footprinting has been expanded by the introduction of modified amino acids photoleucine (L-2-amino-4,4-azipentanoic acid, abbreviated as L*) and photomethionine (L-2-amino-5,5-azihexanoic acid, abbreviated as M*). These not only provide the diazirine photochemical label, but can also be incorporated as amino acid residues into synthetic or cell-expressed proteins where their steric properties closely resemble those of the respective natural residues leucine and methionine [2].

Electronic supplementary material The online version of this article (doi:10.1007/s13361-016-1390-4) contains supplementary material, which is available to authorized users.

Correspondence to: František Tureček; *e-mail:* turecek@chem.washington.edu

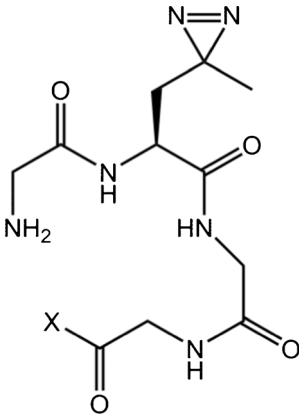

X = NH_2: GL*GG-amide
X = OH: GL*GG

The gas-phase chemistry of photoleucine and photomethionine-containing peptide ions has been studied with the aim to understand their properties [3, 4] and exploit their photochemistry for peptide-ligand footprinting in gas-phase ion–molecule complexes [5, 6]. Collision-induced dissociation under slow heating conditions of singly and doubly charged L*- and M*-tagged peptide ions proceeds by competing loss of N_2 and backbone dissociations [3]. Electron transfer dissociation (ETD) [7] of L*- and M*-tagged peptide ions results in competing backbone dissociations and radical reactions involving the diazirine ring [8, 9]. The L* residue has been calculated to have a substantial electron affinity that facilitates electron attachment in the diazirine ring and triggers proton and hydrogen atom migrations in the charge-reduced peptide ions [8].

One question that has not been addressed by the previous studies was whether the diazirine ring survives intact in backbone fragments produced by ETD. Owing to the substantial excitation energy involved in electron transfer to multiply charged peptide ions [10], one can presume that the diazirine ring may undergo thermal or radical induced rearrangements to stoichiometrically equivalent but structurally different isomers. The activation energy for thermal diazirine-diazo ring opening in the GL*GGK-amide cation (124 kJ mol^{-1}) [3] is well below the excitation energy acquired by ETD in fragment ions of comparable size (240 kJ mol^{-1}) [10] to drive isomerization. Here, we use near-UV photodissociation (UVPD) and infrared multiphoton dissociation (IRMPD) action spectroscopy to investigate the structures and dissociations of GL*GG-amide ions produced as $\boldsymbol{c_4}$ fragments by ETD of doubly and multiply charged peptide ions containing the GL*GG sequence motif. These are compared with authentic GL*GG-amide and GL*GG-tetrapeptide ions. The experimental results are interpreted with the help of extensive ab initio and density functional theory calculations. We wish to demonstrate that the L*-diazirine ring survives backbone dissociation upon ETD of peptide ions.

Experimental

Materials

Photoleucine containing peptides GL*GG, and GL*GGK were synthesized using standard solid phase methods for Wang resin [11]. GL*GG-amide was synthesized on PAL resin. Photoleucine (Pierce Biotechnology, Rockford, IL, USA) was incorporated using standard Fmoc technology [12]. The larger L*-tagged pentacosapeptide, GL*GGKKYTVSIN GGKKITVSIGLLG, was synthesized by Dr. Mathias Schafer (Institute of Organic Chemistry, University of Cologne, Germany) and obtained by courtesy of Dr. Andrea Sinz (Martin Luther University, Halle-Wittenberg, Germany). Exhaustive exchange in GL*GG of mobile O-H and N-H protons for deuterium was performed as reported previously [3].

Methods

UVPD spectra were measured on an LTQ-XL ETD linear ion trap (ThermoElectron Fisher, San Jose, CA, USA) that was equipped with a Nd-YAG laser (EKSPLA, NL 301 HT) providing the third harmonics line at 355 nm of 3–6 ns pulse width and 15 mJ/pulse light intensity. For experimental details of the tandem ETD-UVPD experiments see [5]. Peptide ions were produced by electrospraying 5–10 μmol L^{-1} solutions in 50:50 methanol–water at a 2.0 μL min^{-1} flow rate. An open home-built microspray ion source was used to allow for efficient H/D exchange and isotope measurements [3]. The transfer capillary to the vacuum system was maintained at 180 °C. The ions were mass-isolated with one mass unit wide bandwidth to reject isotope satellites, stored in the ion trap, and probed by a combination of ETD, CID, and UVPD.

IRMPD Spectroscopy

The IRMPD experiment is based on a commercial quadrupole ion trap mass spectrometer (AmaZon Speed ETD, Bruker Daltonik, Bremen, Germany) coupled to the IR beam line of the FELIX free electron laser (FEL) that has been described in more detail elsewhere. Briefly, $[M + 2H]^{2+}$ peptide ions were generated by electrospray ionization from 1–10 μmol L^{-1} peptide solutions in 50:50 acetonitrile:water, ~0.1% formic acid [GeneCust (Luxemburg), 95% purity] that were introduced at 120 μL h^{-1} flow rates and aided by a pressurized nebulizing gas (N_2). In ETD experiments, ions were accumulated, mass isolated, and then reacted with fluoranthene radical anions for ~200 ms. A fragment ion of interest was mass isolated in a subsequent MS/MS stage and irradiated by the tunable infrared beam from the FEL in a final MS/MS stage. FELIX produces infrared radiation in 5–10 μs macropulses at 5 Hz having approximately 30–60 mJ pulse energy (bandwidth ~0.4% of the center frequency). Resonant absorption of infrared radiation followed by intramolecular vibrational redistribution (IVR) of the absorbed energy increases the internal energy of the system and eventually leads to unimolecular dissociation. This produces frequency-dependent fragment ion

intensities, which can be related to parent ion intensity by the yield [yield = ΣI(fragment ions)/ΣI(parent + fragment ions)] and can be used to generate an infrared action spectrum. The yield at each IR point is obtained from four averaged mass spectra. A linear correction for laser power is used and the frequency is calibrated using a grating spectrometer.

Calculations

Conformational search of GL*GG-amide ions was performed according to a previously reported procedure [13]. First, GLGG-amide ions were generated by the ConformSearch engine [13] that rapidly converged to yield 20 low-energy ion conformers. In these, a methyl group in each leucine residue was rebuilt into an L* diazirine ring, and the conformers were fully optimized using DFT gradient optimization. The optimized geometries in a Cartesian coordinate format are given in the Supplementary Tables S1–S8 (in Supporting Information) and are also available from the corresponding author upon request. Standard ab initio and density functional theory (DFT) calculations were performed using the Gaussian 09 suite of programs [14]. Geometry optimizations and harmonic frequency analysis were performed with the hybrid B3LYP [15] and M06-2X [16] functionals using the 6-31+G(d,p) basis set. Entropies were evaluated using corrections for hindered rotors available in Gaussian 09 [14]. Single point energies were calculated with B3LYP, M06-2X, and Moller-Plesset perturbational treatment [17] (MP2, frozen core) using the 6-311++G(2d,p) basis set. At the highest level of theory, single-point energy coupled-cluster calculations [18] with single, double, and disconnected triple excitations [19] were carried out with the 6-31G(d) basis set and the energies were expanded to the CCSD(T)/6-311++G(3df,2p) level using the standard linear extrapolation formula: E[CCSD(T)/6-311++G(3df,2p)] ≈ E[CCSD(T)/6-31G(d)] + E[MP2/6-311++G(3df,2p)] − E[MP2/6-31G(d)]. The GL*GG-amide ion relative energies are presented in Supplementary Table S9. Singlet excited-state energies and oscillator strengths for vertical excitations were calculated for select ion conformers using time-dependent DFT (TD-DFT) with the M06-2X and ωB97X-D [20] functionals and the 6-311++G(2d,p) basis set. Rice-Ramsperger-Kassel-Marcus (RRKM) calculations of unimolecular rate constants were performed as described previously [21, 22].

Results

To characterize the $\boldsymbol{c_4}$ ions (*m/z* 314) produced from GL*GGX peptide ion precursors, we first analyze their ETD-CID-MS^3 spectra and compare them with CID-MS^2 spectra of reference *m/z* 314 ions directly generated by electrospray ionization of GL*GG-amide. The $\boldsymbol{c_4}$ ion was generated by ETD of the +4 charge state of GL*GGKKYTVSINGGKKITVSIGLLG (*m/z* 619) or from the +2 charge state of GL*GGK (*m/z* 222) [3], and its identity was unequivocally confirmed by accurate mass measurements under high-resolution conditions ($m/\Delta m$ = 120,000, *m/z* 314.1566, $C_{11}H_{20}N_7O_4^+$ requires *m/z* 314.1571). The ETD spectra of both peptide ions are given in Supplementary Figure S1a, b (in Supporting Information). The CID spectra of the $\boldsymbol{c_4}$ ions generated from both of the GL*GGX peptide ions were indistinguishable as far as the fragment ion intensities were concerned and virtually identical to the CID spectrum of the reference ion of protonated GL*GG amide (Figure 1a–c). A conspicuous feature of all these spectra was the extremely low intensity of the *m/z* 286 fragment ion formed by collision-induced elimination of N_2. This dissociation is typical for CID of L*-containing peptide ions, where it proceeds via thermally induced diazirine isomerization to a diazoalkane intermediate [3]. Loss of N_2 from diazoalkanes is promoted by protonation and depends on the presence of a suitable proton donor in the gas-phase ion [3]. This is illustrated by the CID-MS^3 spectra of larger $\boldsymbol{c}$ fragment ions from ETD of the pentacosapeptide 4+ ion, which formally correspond to protonated GL*GGK-amide ($\boldsymbol{c_5}$, *m/z* 442) GL*GGKK-amide ($\boldsymbol{c_6}$, *m/z* 570), and GL*GGKKY-amide ions ($\boldsymbol{c_7}$, *m/z* 733) (Supplementary Figure S2a–c). All these $\boldsymbol{c}$ ions contain lysine residues as the likely protonation sites and undergo very efficient and dominant loss of N_2 upon CID.

Two other related experiments were carried out to bear on the question of N_2 loss. The $[GL^*GG + H]^+$ ion (*m/z* 315) and its d_7-isotopologue (*m/z* 322 by complete H/D exchange) were generated and their CID spectra were recorded (Figure 2a, b). These peptide ions again showed very minor fragment ions formed by loss of N_2 from the diazirine ring, the dominant dissociation being loss of water (*m/z* 297). However, the major fragment ions at *m/z* 297, *m/z* 240 ($\boldsymbol{b_3}$), and *m/z* 183 ($\boldsymbol{b_2}$) were accompanied by lower-mass satellites at a mass difference of −28.0061 Da, indicating a loss of N_2.

The distribution of exchangeable deuterium atoms in the CID fragments of the *m/z* 322 ion showed differences (Figure 2b). Fragments formed by loss of water (*m/z* 302) and consecutive loss of N_2 (*m/z* 274) were all d_5 species, consistent with elimination of D_2O incorporating exchangeable protons only. The $(\boldsymbol{y_3} - N_2)^+$ fragment ion cleanly retained six deuterium atoms as illustrated by the *m/z* 230 → *m/z* 236 mass shift, which was consistent with its formation by a transfer of two exchangeable protons from the Gly-1 residue. By contrast, the $\boldsymbol{b_2}$ and $\boldsymbol{y_2}$ fragment ions showed incomplete deuterium content (d_1–d_3 and d_1–d_5, respectively), which indicated H/D exchange between the O,N−D and C−H atoms in these ions in the course of fragmentation. Most conspicuously, the *m/z* 155 $(\boldsymbol{b_2} - N_2)^+$ satellite of the $\boldsymbol{b_2}$ ion showed d_3 and d_4 species upon deuteration, which was incompatible with it being formed by consecutive loss of N_2 from the $\boldsymbol{b_2}$ precursor which had a quite different isotope distribution that lacked a d_4 species.

In another related experiment, a noncovalent complex of the $\boldsymbol{c_4}$ ion and 18-crown-6-ether [$\boldsymbol{c_4}$(CE), *m/z* 578] was generated by ETD of the GL*GGK-crown ether complex, $(GL^*GGK + CE + 2H)^{2+}$, and probed by CID and UVPD. Complexation with the crown ether involves hydrogen bonding to the charged peptide group [23–27], which is effectively shielded from engaging in proton transfer within the peptide moiety. The

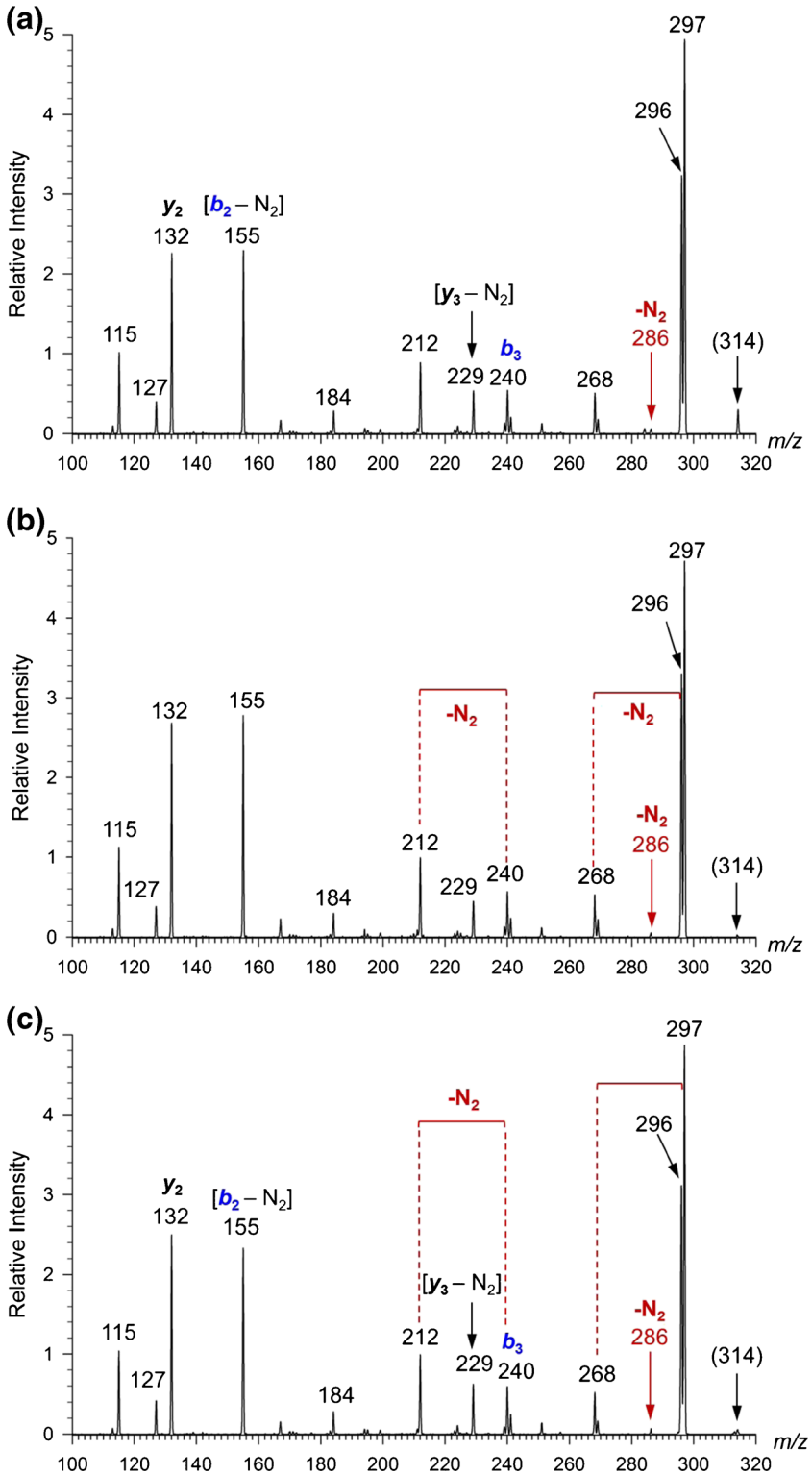

Figure 1. CID-MS^3 spectra of *m/z* 314 ions from **(a)** GL*GG-amide, **(b)** c_4 ETD fragment ion from GL*GGKKYTVSINGGKKITVSIGLLG, and **(c)** c_4 ETD fragment ion from GL*GGK

CID spectrum of the c_4(CE) ion showed a dominant loss of CE (*m/z* 314) in combination with elimination of N_2 (*m/z* 286) (Figure 3a). In contrast, collision-induced loss of N_2 produced only a very minor fragment ion at *m/z* 550 (Figure 3a). This dramatically differs from UVPD of the c_4(CE) ion (Figure 3b) that shows consecutive loss of N_2 (*m/z* 550) and the crown ether ligand (CE)(*m/z* 286) but no direct loss of CE from the complex (*m/z* 314).

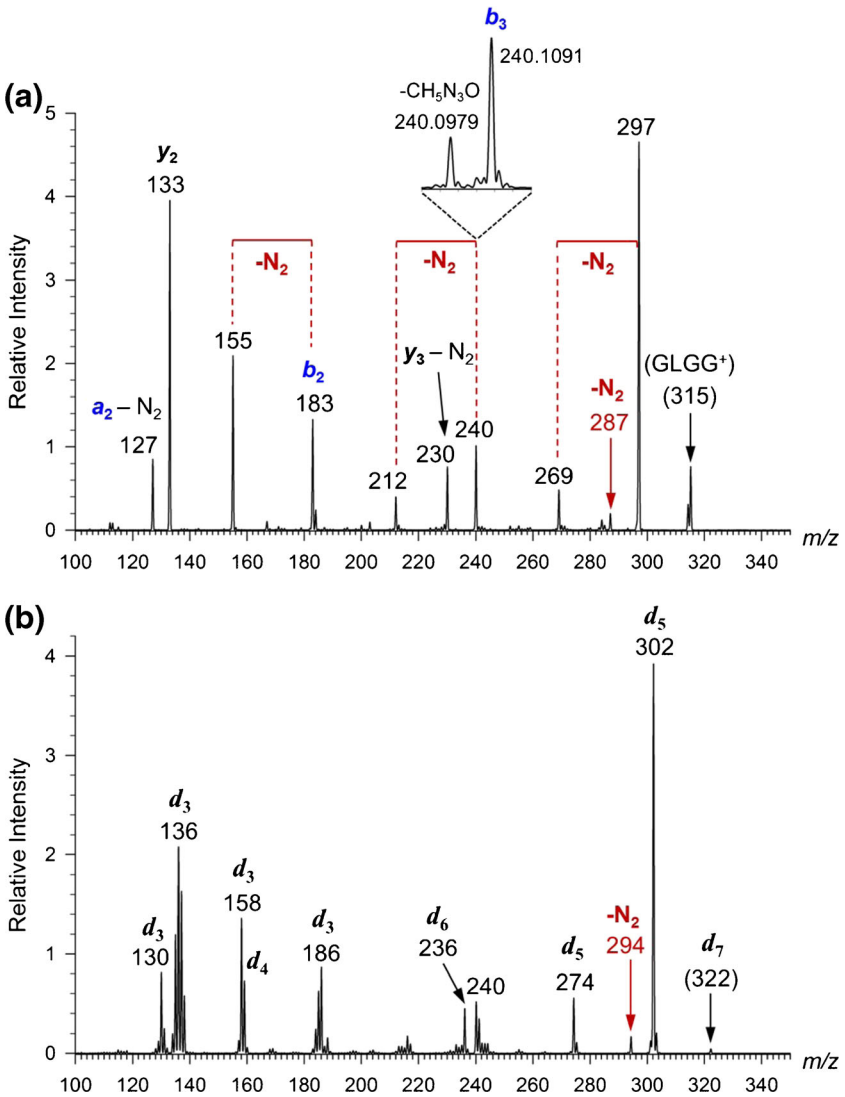

Figure 2. CID-MS^3 spectra of *m/z* 315 ions from **(a)** (GL*GG + H)$^+$, and **(b)** completely H/D exchanged ion (d_6-GL*GG + D)$^+$

Near-UV Photodissociation

The diazirine ring is a distinct albeit weak chromophore that absorbs light and undergoes photodissociation in a region of the spectrum where natural peptide chromophores are transparent and do not interfere. Loss of N_2 is the only primary photodissociation channel of diazirines whereas isomers, such as diazoalkanes that could be formed by thermal rearrangement of diazirines, do not absorb light at 355 nm [28]. This contrasts CID where loss of N_2 can signify diazirine or diazoalkane structures [3]. Irradiation of the ETD-produced $\boldsymbol{c_4}$ ion resulted in photodissociation, indicating the presence in the ion of a chromophore absorbing light at 355 nm. The UVPD spectrum (Figure 4a) showed backbone fragment ions lacking N_2, *m/z* 229, 212, and 155, which were analogous to those in the CID spectrum (Figure 1a). In contrast, N_2-containing fragment ions and those formed by loss of ammonia and water (*m/z* 297 and 296, respectively) were extremely weak. This is consistent with the presence of a diazirine ring that undergoes photolysis and N_2 expulsion followed by backbone dissociation of the primary fragment ions. However, these are not detectable at *m/z* 286 in the UVPD spectrum and thus must undergo very facile dissociation.

The related GL*GG ion showed a similar UVPD spectrum (Figure 4b). Photodissociation of the diazirine ring chiefly formed backbone fragment ions that eliminated N_2, e.g., $(\boldsymbol{y_3} - N_2)^+$, $(\boldsymbol{b_2} - N_2)^+$, and $(\boldsymbol{a_2} - N_2)^+$, at *m/z* 230, 155, and 127, respectively. The *m/z* 287 ion by direct loss of N_2 was weak, as were the N_2-containing $\boldsymbol{b_3}$ and $\boldsymbol{b_2}$ fragment ions at *m/z* 240 and 183, respectively. A plot of ion relative intensities as a function of laser pulses (Supplementary Figure S3a) showed an exponential depletion of the the GL*GG ion relative intensity according to the formula: $I/I_0 = e^{-0.05523n}$ where n is the number of laser pulses. The small value of the exponent is consistent with the weak absorption of diazirine at 355 nm. The relative intensities of both the major (Supplementary Figure S3a) and minor (Supplementary Figure S3b) photofragment ions did not appreciably change upon increasing the number of laser pulses.

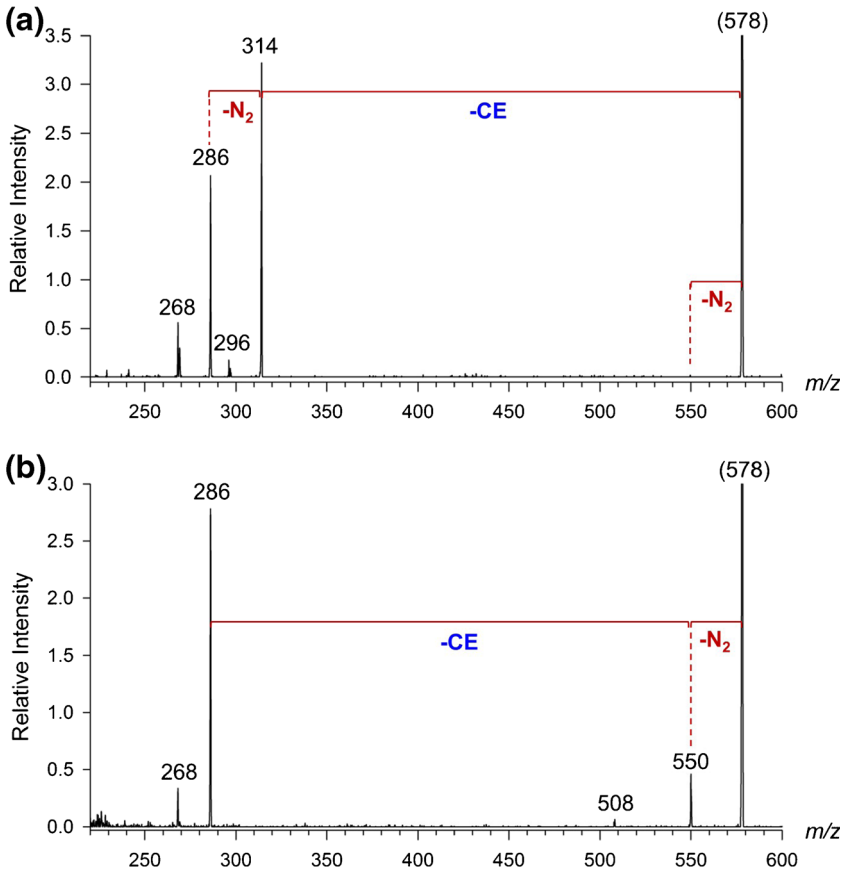

Figure 3. **(a)** ETD-CID-MS^3 and **(b)** ETD-UVPD-MS^3 spectra of $\boldsymbol{c_4}$-crown ether complex (*m/z* 578)

All these experimental data indicated that the GL*GG ion population was homogeneous, consisting of species that contained the diazirine ring as the only chromophore.

IRMPD Action Spectroscopy of $\boldsymbol{c_4}$ Ions

The $\boldsymbol{c_4}$ ions from ETD of GL*GGK were further characterized by infrared multiphoton photodissociation (IRMPD) action spectroscopy in the finger print region (1000–1800 cm^{-1}, Figure 5) and also in an extended 2000–2400 cm^{-1} region to search for the presence of a C=N=N diazoalkane group. The IRMPD action spectrum is shown in Figure 5. The 2000–2400 cm^{-1} region showed no absorption. This excluded the diazoalkane group, C=N=N, for which a strong absorption was expected at 2100 cm^{-1} (ion **8** in Figure 5). Since the 2000–2400 cm^{-1} region is not frequently explored in IRMPD experiments, the photodissociation efficiency was checked with a control experiment of IRMPD of an ionized isocyanate, 4-(4-isocyanatopyrid-2-yl)morpholine. The spectrum (Supplementary Figure S4) showed a strong photodissociation band because of absorption by the N=C=O stretching mode at 2260 cm^{-1}. This suggests that a C=N=N group, which is another strong IR chromophore (ν = 2100 cm^{-1}, 534 km mol^{-1}), would have been detected had it been present in the peptide ion. The calculated spectra also indicate that the diazirine-related vibration modes, the ν(N=N) stretch at 1672 cm^{-1} and the symmetrical N-C-N ring stretching mode at 1198 cm^{-1}, are both too weak (the respective calculated IR intensities for **1** were 35 and 22 km mol^{-1}, Supplementary Table S10) and overlapping with other modes to be of diagnostic value.

The IRMPD spectrum of the $\boldsymbol{c_4}$ ion in Figure 5 was assigned by comparing it with the B3LYP calculated IR absorption spectra of several isomeric structures for low energy GL*GG-amide (**1**–**4**) and GL*GG-enolimine (**5**–**7**) ion tautomers. The optimized ions structures are shown in Figure 6. The B3LYP/6-31+G(d,p) harmonic frequencies were scaled by 0.975 and the absorption lines were broadened by convolution with Gaussian functions at 25 cm^{-1} full width at half maximum (Figure 5). The best match was obtained for diazirine side-chain conformers **1** and **2** of GL*GG-amide. The main distinctive feature of the calculated spectra was the wave number and intensity of the amide NH_2 scissoring vibration, as assigned in Supplementary Table S10, which was coupled to amide ν(C=O) stretching modes. In **1**, these vibrations appear at 1595, 1672, and 1696 cm^{-1} to fit the bands in the IRMPD spectrum. In **3**, these bands are more intense and appear at 1577, 1648, and 1673, changing the band pattern and making it dissimilar with that in the IRMPD spectrum. The calculated spectra also indicate that the diazirine-related vibration modes, the ν(N=N) stretch and the symmetrical N-C-N ring stretching mode, are both too weak and overlapping with other modes to be of diagnostic value.

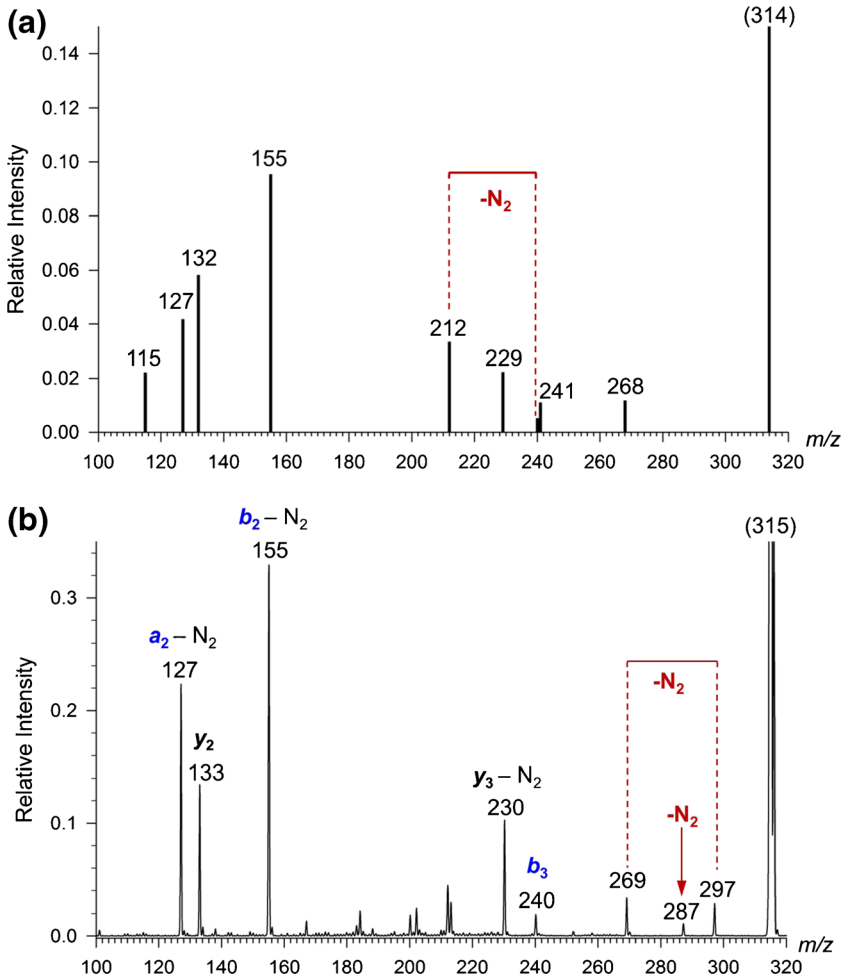

Figure 4. **(a)** ETD-UVPD-MS^3 spectrum of c_4 ion from GL*GGK obtained with seven laser pulses. The fragment ions were extracted from background caused by laser photodesorption-ionization of surface deposits and are presented as bar graphs. **(b)** UVPD-MS^2 spectrum of $(GL^*GG + H)^+$ (*m/z* 315) obtained with a single laser pulse\

The calculated IR spectra clearly distinguish amide tautomers from enolimines. The spectra of enolimine conformers **5** and **6** (Figure 5) show strong bands of δ(C-O-H) in-plane bending modes at 1040–1050 and 1190–1220 cm^{-1}. The former band is missing in the IRMPD spectrum, indicating that enolimines are not significantly represented among the c_4 ion population.

Discussion

The results of near-UV photodissociation and IRMPD jointly point to two major structure features of the c_4 ions produced by ETD. One feature, apparent from the UVPD and IRMPD experiments, is that the diazirine ring survives in L* residues following electrospray ionization and ETD of doubly charged peptide ions. The other feature, revealed by IRMPD, is that these c_4 ions are predominantly amide tautomers. The distinction of diazirine and diazoalkanes isomers by UVPD relies on the calculated absorption bands for the two chromophores. TD-DFT calculations with four density functionals gave very similar excitation energies and oscillator strengths (Supplementary Table S11), the ωB97X-D results are discussed in the text. Diazirine isomer **1** showed a weak transition to the first excited state at 363 nm with a 0.0006 oscillator strength. The pertinent electronic transition in GL*GG-amide consists of a forbidden excitation from the diazirine highest occupied π_{xy} molecular orbital (HOMO, MO83) to the lowest-unoccupied orbital (LUMO, MO84) of a π_z symmetry, as shown for **1** (Supplementary Figure S5). The symmetry-forbidden nature of this transition accounts for the weakly absorbing properties of diazirines [28]. The excitation energy for the first excited state was only weakly dependent on the ion conformation and the presence of carboxyl, amide or enolimine group, showing 3.50 ± 0.06 eV (354 ± 6 nm) from ωB97X-D TD-DFT calculations and likewise for the other DFT methods (Supplementary Table S11). Excitations to the second and higher excited states involve amide π-electrons and appear in the UV region of the spectrum below 230 nm (Supplementary Table S11).

In contrast to the diazirines, TD-DFT calculations of their diazoalkane isomers show a symmetry-forbidden transition to the first excited state at 490 nm of an extremely small oscillator

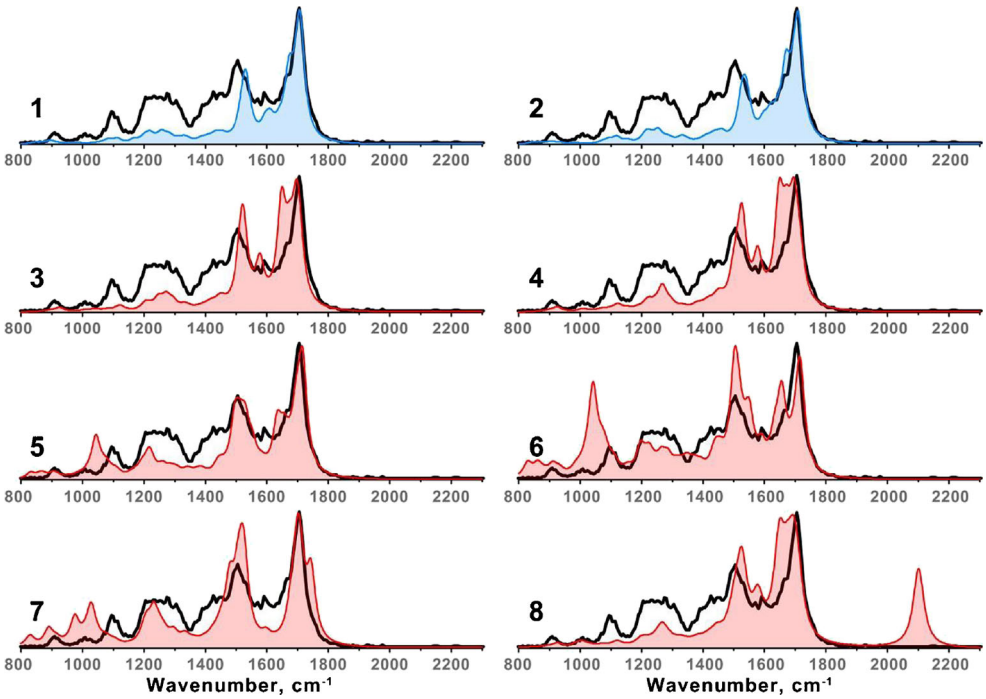

Figure 5. IRMPD action spectrum of the c_4 ion from ETD of $(GL^*GGK + 2H)^{2+}$ (bold line) and B3LYP-6-31+G(d,p)-calculated IR absorption spectra of ions **1**–**8**. Best fits for **1** and **2** are shown with blue outlines and shading, the others are shown in red

strength. The next transition to the second excited state is in the UV region (239 nm), which does not overlap with the diazirine $\pi_{xy} \rightarrow \pi_z^*$ excitation. These features explain why photodissociation at 355 nm is so highly selective for photoleucine and other diazirine-containing tags in peptide ions. IRMPD provides indirect evidence of the diazirine group by excluding the presence of the isomeric diazoalkane chromophore. IRMPD gives convincing evidence for the absence of a C-terminal enolimine group which, eo ipso, indicates that the c_4 ion is a C-terminal amide. This result is consistent with a previous ECD-IRMPD study of a fixed-charge tagged dipeptide where the c_0 fragment ion was also assigned to have a C-terminal amide group [29]. We note that the previous assignment was based on the presence of an amide C=O stretch in the IRMPD action spectrum, which does not present a distinctive feature for larger c ions. Our result for the c_4 ion indicates that the formation of amide isomers may not be restricted to the special case of a small charge-tagged peptide, but could be of general nature. Previous computational studies of ETD fragment ions from GLGGK [30] and other peptide ions [31] found that an isomerization of the enolimine c_1 fragment to its more stable amide form required only a low activation energy and was predicted to be very facile [30, 31]. This prototropic isomerization can occur in an ion–molecule complex and be catalyzed by the protonated lysine group. We presume that a similar isomerization also proceeds in ion–molecule $(c + z)^{+\bullet}$ complexes transiently formed by ETD of GL*GKX ions to produce the more stable amide form of the c fragment, as illustrated for the c_4 ion.

Finally, we discuss the energetics and differences in the collision and UV-induced dissociations of GL*GG and GL*GG amide ions. CID of GL*GG-amide and c_4 ions shows competitive eliminations of ammonia, water, diazirine, nitrogen, and backbone dissociations (Figure 1a–c).

The loss of N_2 can be used as an energy reference (thermometer) dissociation for which we determined the activation energy as E(TS) = 135 kJ mol^{-1} and dissociation threshold of 46 kJ mol^{-1} in **1** from ab initio calculations at the CCSD(T)/6-311++G(3df,2p) high level of theory. The reaction proceeds through mildly exothermic ring opening to a diazoalkane isomer ($\Delta E = -15$ kJ mol^{-1}) that readily eliminates N_2 [3]. The fact that the loss of water, ammonia, and backbone dissociations compete with loss of N_2 indicates that they have similar activation energies. Furthermore, the loss of N_2 is accompanied by a highly exothermic isomerization of the $(MH - N_2)^+$ ion from a carbene intermediate to a more stable alkene or cyclic isomers [3]. This potential energy drop of >200 kJ mol^{-1}supplies internal excitation for the $(MH - N_2)^+$ ion to undergo backbone dissociations forming the denitrogenated $(b_2 - N_2)^+$ and $(y_3 - N_2)^+$ fragment ions (Figure 1a–c). Interestingly, the c_4 ion from ETD of GL*GGK shows ca. 33% of spontaneous dissociation forming secondary fragment ions identical to those in the CID spectrum of GL*GG-amide (Supplementary Figure S6). Using unimolecular rate constants calculated by RRKM on the CCSD(T)/6-311++G(3df,2p) potential energy surface (Supplementary Figure S7), we can estimate the mean internal energy of the ETD-formed c_4 ion as 280 kJ mol^{-1}. This estimate is in the same range as the ETD fragment ion energies determined by the recent kinetic ion thermometer study of peptide ions [10]. That only 33% of the c_4 ion dissociates on the 200 ms time scale of the ETD measurement can be attributed to

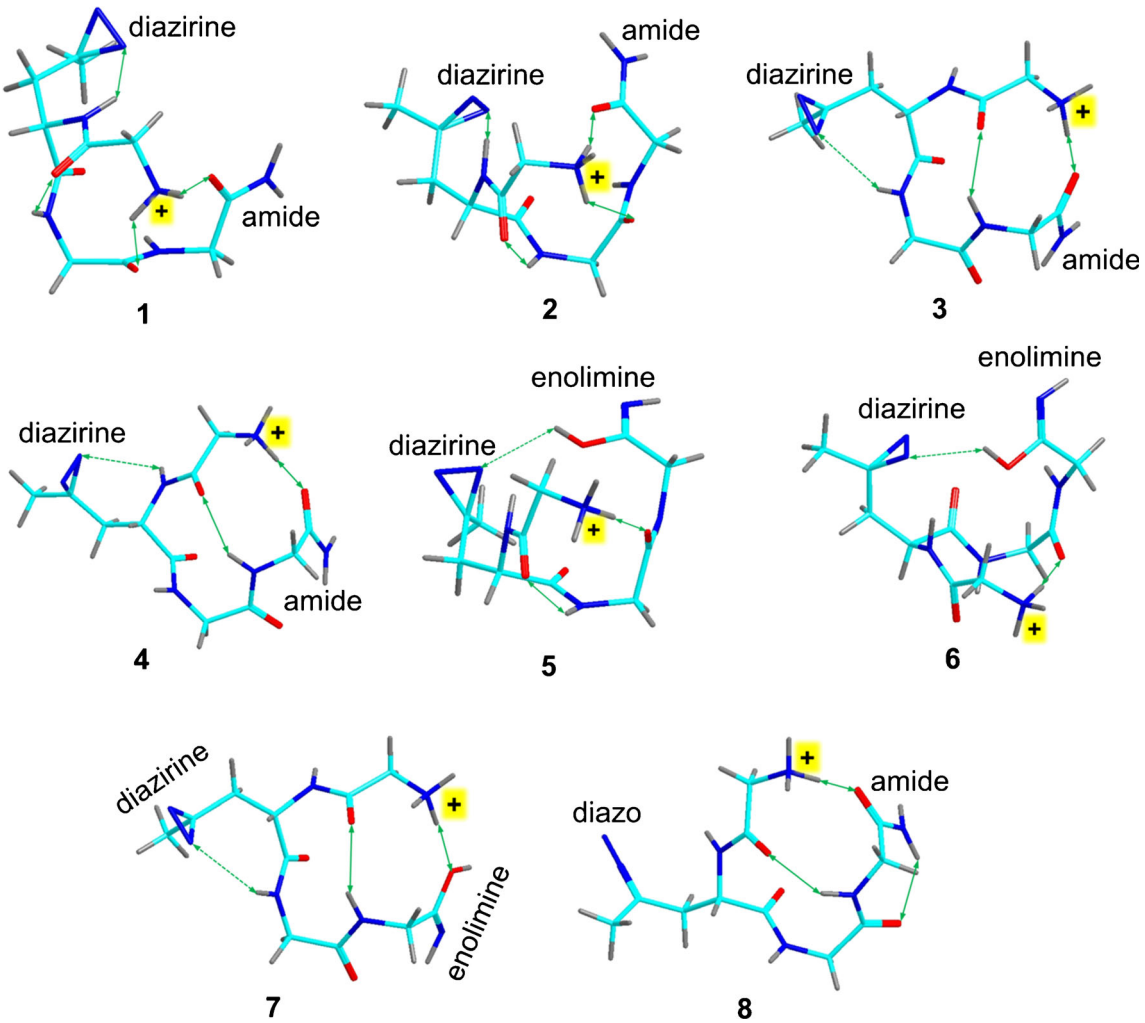

Figure 6. B3LYP/6-31+G(d,p) optimized structures of ions **1**–**8**. Atom color coding is as follows: cyan = C, red = O, blue = N, gray = H. Green double-ended arrows indicate hydrogen bonds

efficient collisional cooling of the fragment ions that are de-excited within 20 ms [10].

In contrast to nonspecific excitation by slow-heating upon CID, UVPD selectively generates the carbene intermediate by electronic excitation of the diazirine ring. The UVPD spectra show that this results in a suppression of the competing dissociations by loss of water, ammonia, and backbone dissociations in GL*GG-amide and GL*GG (Figure 4a, b). The fragmentation after photodissociative expulsion of N_2 starts from the $(MH - N_2)^+$ ion and shows only a minor loss of water whereas the formation of denitrogenated backbone fragments is predominant. The energetics of UVPD includes absorption of a 3.493 eV (337 kJ mol^{-1}) photon that cleaves the diazirine ring. The carbene-forming loss of N_2 is 60–80 kJ mol^{-1} endothermic on the potential energy of the singlet ground state [3], and the excess energy balance of 260–280 kJ mol^{-1} is partitioned between the kinetic, vibrational, and rotational energy of the departing N_2 molecule and the internal energy of the $(MH - N_2)^+$ ion. However, the partition ratio determining the internal energy of the peptide carbene is unknown, and a further excitation of the ion is provided by exothermic carbene isomerization. This proceeds very rapidly, as the rate constants for alkyl carbene isomerizations to olefins are in the 10^8–10^9 s^{-1} range [32–34], and so the peptide carbene is too short-lived to be collisionally cooled. The dominant formation upon UVPD of small fragments, such as $(\boldsymbol{a_2} - N_2)^+$, $(\boldsymbol{b_2} - N_2)^+$ and $\boldsymbol{y_2}$, is consistent with UVPD being more energetic than CID.

Conclusions

The results presented in this combined experimental and computational study allow us to arrive at the following conclusions. ETD of peptides containing the photoleucine residue produces fragment ions of the $\boldsymbol{c}$ type that retain intact diazirine rings. This indicates that electron attachment to the peptide ion that results in backbone cleavage close to the photoleucine residue does not involve the electrophilic diazirine moiety. The finding that the $\boldsymbol{c_4}$ ion formed by backbone dissociation of GL*GGK is the more stable amide tautomer can be interpreted by prototropic isomerization in an ion–molecule $(\boldsymbol{c_4} + \boldsymbol{z_1})^{+\bullet}$ complex.

Acknowledgments

Research at University of Washington was supported by a grant from the Chemistry Division of the National Science Foundation, grant CHE-1359810. F.T. thanks Klaus and Mary Ann Saegebarth Endowment for support. The authors thank Dr. Mathias Schafer (Institute of Organic Chemistry, University of Cologne, Germany) and Dr. Andrea Sinz (Martin Luther University, Halle-Wittenberg, Germany) for the sample of the L*-labeled pentacosapeptide. The authors gratefully acknowledge the FELIX staff, particularly Dr. B. Redlich and Dr. A.F.G. van der Meer for technical support. The work at the FELIX laboratory was financially supported by NWO Chemical Sciences under VICI project no. 724.011.002 awarded to J.O. This work is part of the research program of FOM, which is financially supported by NWO.

References

1. Das, J.: Aliphatic diazirines as photoaffinity probes for proteins: Recent developments. Chem. Rev. **111**, 4405–4417 (2011)
2. Suchanek, M., Radzikowska, A., Thiele, C.: Photo-leucine and photo-methionine allow identification of protein–protein interactions in living cells. Nat. Methods **2**, 261–268 (2005)
3. Marek, A., Tureček, F.: Collision-induced dissociation of diazirine-labeled peptide ions. Evidence for Brønsted-acid assisted elimination of nitrogen. J. Am. Soc. Mass Spectrom. **25**, 779–789 (2014)
4. Koelbel, K., Ihling, C.H., Sinz, A.: Analysis of peptide secondary structures by photoactivatable amino acid analogues. Angew. Chem. Int. Ed. **51**, 12602–12605 (2012)
5. Shaffer, C.J., Marek, A., Pepin, R., Slováková, K., Tureček, F.: Combining UV photodissociation with electron transfer for peptide structure analysis. J. Mass Spectrom. **50**, 470–475 (2015)
6. Shaffer, C.J., Andrikopoulos, P.C., Řezáč, J., Rulíšek, L., Tureček, F.: Efficient covalent bond formation in gas-phase peptide–peptide ion complexes with the photo-leucine stapler. J. Am. Soc. Mass Spectrom. **27**, 633–645 (2016)
7. Syka, J.E.P., Coon, J.J., Schroeder, M.J., Shabanowitz, J., Hunt, D.F.: Peptide and protein sequence analysis by electron transfer dissociation mass spectrometry. Proc. Natl. Acad. Sci. U. S. A. **101**, 9528–9533 (2004)
8. Marek, A., Pepin, R., Peng, B., Laszlo, K.J., Bush, M.F., Tureček, F.: Electron transfer dissociation of photolabeled peptides. Backbone cleavages compete with diazirine ring rearrangements. J. Am. Soc. Mass Spectrom. **24**, 1641–1653 (2013)
9. Shaffer, C.J., Marek, A., Nguyen, H.T.H., Tureček, F.: Combining near-UV photodissociation with electron transfer. Reduction of the diazirine ring in a photomethionine- labeled peptide ion. J. Am. Soc. Mass Spectrom. **26**, 1367–1381 (2015)
10. Pepin, R., Tureček, F.: Kinetic ion thermometers for electron transfer dissociation. J. Phys. Chem. B **119**, 2818–2826 (2015)
11. Janz, J.M., Ren, Y., Looby, R., Kazmi, M.A., Sachdev, P., Grunbeck, A., Haggis, L., Chinnapen, D., Lin, A.Y., Seibert, C., McMurry, T., Carlson, K.E., Muir, T.W., Hunt, S., Sakmar, T.P.: Direct interaction between an allosteric agonist pepducin and the chemokine receptor CXCR4. J. Am. Chem. Soc. **133**, 15878–15881 (2011)
12. Coste, J., LeNguyen, D., Castro, B.: PyBOP: A new peptide coupling reagent devoid of toxic by-product. Tetrahedron Lett. **31**, 205–208 (1990)
13. Moss, C.L., Chamot-Rooke, J., Brown, J., Campuzano, I., Richardson, K., Williams, J., Bush, M., Bythell, B., Paizs, B., Tureček, F.: Assigning structures to gas-phase peptide cations and cation-radicals. An infrared multiphoton dissociation, ion mobility, electron transfer, and computational study of a histidine peptide ion. J. Phys. Chem. B **116**, 3445–3456 (2012)
14. Frisch, M.J., Trucks, G.W., Schlegel, H.B., Scuseria, G.E., Robb, M.A., Cheeseman, J.R., Scalmani, G., Barone, V., Mennucci, B., Petersson, G.A., Nakatsuji, H., Caricato, M., Li, X., Hratchian, H.P., Izmaylov, A.F., Bloino, J., Zheng, G., Sonnenberg, J.L., Hada, M., Ehara, M., Toyota, K., Fukuda, R., Hasegawa, J., Ishida, M., Nakajima, T., Honda, Y., Kitao, O., Nakai, H., Vreven, T., Montgomery Jr., J.A., Peralta, J.E., Ogliaro, F., Bearpark, M., Heyd, J.J., Brothers, E., Kudin, K.N., Staroverov, V.N., Kobayashi, R., Normand, J., Raghavachari, K., Rendell, A., Burant, J.C., Iyengar, S.S., Tomasi, J., Cossi, M., Rega, N., Millam, J.M., Klene, M., Knox, J.E., Cross, J.B., Bakken, V., Adamo, C., Jaramillo, J., Gomperts, R., Stratmann, R.E., Yazyev, O., Austin, A.J., Cammi, R., Pomelli, C., Ochterski, J.W., Martin, R.L., Morokuma, K., Zakrzewski, V.G., Voth, G.A., Salvador, P., Dannenberg, J.J., Dapprich, S., Daniels, A.D., Farkas, O., Foresman, J.B., Ortiz, J.V., Cioslowski, J., Fox, D.J.: Gaussian 09, Revision A.02. Gaussian, Inc, Wallingford (2009)
15. Becke, A.D.: A new mixing of Hartree-Fock and local density-functional theories. J. Chem. Phys. **98**, 1372–1377 (1993)
16. Zhao, Y., Truhlar, D.G.: The M06 suite of density functionals for main group thermochemistry, thermochemical kinetics, noncovalent interactions, excited states, and transition elements: Two new functionals and systematic testing of four M06-class functionals and 12 other functionals. Theor. Chem. Acc. **120**, 215–241 (2008)
17. Møller, C., Plesset, M.S.: A note on an approximation treatment for many-electron systems. Phys. Rev. **46**, 618–622 (1934)
18. Čížek, J., Paldus, J., Šroubková, L.: Cluster expansion analysis for delocalized systems. Int. J. Quantum Chem. **3**, 149–167 (1969)
19. Purvis, G.D., Bartlett, R.J.: A full coupled-cluster singles and doubles model. The inclusion of disconnected triples. J. Chem. Phys. **76**, 1910–1918 (1982)
20. Chai, J.D., Head-Gordon, M.: Long-range corrected hybrid density functionals with damped atom-atom dispersion corrections. Phys. Chem. Chem. Phys. **10**, 6615–6620 (2008)
21. Ledvina, A.R., Chung, T.W., Hui, R., Coon, J.J., Tureček, F.: Cascade dissociations of peptide cation-radicals. Part 2. Infrared multiphoton dissociation and mechanistic studies of z- ions from pentapeptides. J. Am. Soc. Mass Spectrom. **23**, 1351–1363 (2012)
22. Frank, A.J., Sadílek, M., Ferrier, J.G., Tureček, F.: Sulfur oxoacids and radicals in the gas phase. A variable-time neutralization-photoexcitation-reionization mass spectrometric and ab initio/RRKM study. J. Am. Chem. Soc. **119**, 123–143 (1997)
23. Haag, N., Holm, A.I.S., Johansson, H.A.B., Zettergren, H., Schmidt, H.T., Nielsen, S.B., Hvelplund, P., Cederquist, H.: Electron capture induced dissociation of doubly protonated pentapeptides: Dependence on molecular structure and charge separation. J. Chem. Phys. **134**, 035102/1–035102/6 (2011)
24. Ly, T., Julian, R.R.: Using ESI-MS to probe protein structure by site-specific noncovalent attachment of 18-Crown-6. J. Am. Soc. Mass Spectrom. **17**, 1209–1215 (2006)
25. David, W.M., Brodbelt, J.S.: Threshold dissociation energies of protonated amine/polyether complexes in a quadrupole ion trap. J. Am. Soc. Mass Spectrom. **14**, 383–392 (2003)
26. Tao, Y., Julian, R.R.: Examining protein surface structure in highly conserved sequence variants with mass spectrometry. Biochemistry **51**, 1796–1802 (2012)
27. Julian, R.R., Beauchamp, J.L.: Site specific sequestering and stabilization of charge in peptides by supramolecular adduct formation with 18-crown-6 ether by way of electrospray ionization. Int. J. Mass Spectrom. **210**, 613–623 (2001)
28. Liu, M.T.H.: Chemistry of Diazirines, Vol. I and II. CRC Press, Boca Raton, FL (1987)
29. Frison, G., Bull, A., van der Rest, G., Tureček, F., Besson, T., Lemaire, J., Maître, P., Chamot-Rooke, J.: Structure of ECD fragments from charge-tagged peptides probed by tunable IRMPD. J. Am. Chem. Soc. **130**, 14916–14917 (2008)
30. Pepin, R., Laszlo, K.J., Peng, B., Marek, A., Bush, M.F., Tureček, F.: Comprehensive analysis of Gly-Leu-Gly-Gly-Lys peptide dication structures and cation-radical dissociations following electron transfer: from electron attachment to backbone cleavage, ion–molecule complexes and fragment separation. J. Phys. Chem. A **118**, 308–324 (2014)
31. Bythell, B.J.: To jump or not to jump? C-alpha hydrogen atom transfer in post-cleavage radical-cation complexes. J. Phys. Chem. A **117**, 1189–1196 (2013)
32. Jackson, J.E., Soundararajan, N., Whie, W., Liu, M.T.H., Bonneau, R., Platz, M.S.: Measurement of the absolute rate of 1,2-hydrogen migration in benzylchlorocarbene. J. Am. Chem. Soc. **111**, 6874–6875 (1989)
33. Pezacki, J.P., Couture, P., Dunn, J.A., Warkentin, J., Wood, P.D., Lusztyk, J., Ford, F., Platz, M.S.: Rate constants for 1,2-hydrogen migration in cyclohexylidene and in substituted cyclohexylidenes. J. Org. Chem. **64**, 4456–4464 (1999)
34. Stevens, I.D.R., Liu, M.T.H., Soundararajan, N., Paike, N.: The barrier for 1,2 hydrogen shift in dialkyl carbenes. Tetrahedron Lett. **30**, 481–484 (1989)